Ceramics International xxx (xxxx) xxx–xxx

Contents lists available at ScienceDirect

Ceramics International

journal homepage: www.elsevier.com/locate/ceramint

Ambient weathering of steelmaking ladle slags

Marcos N. Moliné[a], Walter A. Calvo[a], Analía G. Tomba Martinez[a,*], Pablo G. Galliano[b]

[a] Instituto de Investigaciones en Ciencia y Tecnología de Materiales (INTEMA), CONICET-Facultad de Ingeniería/Universidad Nacional de Mar del Plata, Av. Colón 10850, 7600 Mar del Plata, Argentina

[b] Tenaris SIDERCA, Dr Simini 250, 2804 Campana, Argentina

ARTICLE INFO

Keywords:
C. Chemical properties
Ladle slag weathering

ABSTRACT

During cooling and permanence outside, the solidified slag involved in the refinement process taking place in the steelmaking ladles suffers attack by environmental components such as water vapor and gaseous CO_2 (weathering). The reactions involved are hydration and carbonation, and as a consequence, the pulverization of the slag occurs. In the present paper, the results of a study of the degradation of a typical steelmaking ladle slag over a period of eighteen weeks (126 days) are reported. To monitor the slag evolution, several experimental techniques were used, some of them rarely employed in this context, after dividing the initial slag batch in four granulometric fractions between > 7.2 mm and < 1.4 mm: granulometry by sieving, X-ray fluorescence (XRF), X-ray diffraction (XRD), and thermogravimetric (TGA) and thermal differential (DTA) analyses. As was already known, the main elements responsible for the slag degradation are free lime, followed by calcium aluminates and magnesia. It was also found that anhydrous and hydrated calcium aluminates are concentrated in the finest granulometric fractions and contribute to the generation of fines mainly during the final stage of hydration. The high percentage of particles smaller than 1.4 mm, with cementitious properties provided mainly by the presence of anhydrous calcium aluminates, are promising characteristics for alternative reusing of the studied ladle slag. Furthermore, slag weathering mechanisms are critical for understanding other steelmaking processes in which the slag is deeply involved, such as the protective role of the remaining thin slag layer against decarburation of ladle or converter working lining refractory bricks.

1. Introduction

The steelmaking slag formed in the ladle, where the secondary metallurgy occurs (and the final steel chemical composition is adjusted), is known as *white slag* or LFS (Ladle Furnace Slag). At operating temperature (1600–1700 °C), this slag floats over the liquid metal, and continuous stirring by argon gas blowing helps displacing the impurities from the metal to the molten slag. The composition of the white slag is varied, although it generally includes calcia (CaO), alumina (Al_2O_3), silica (SiO_2) and magnesia (MgO). Moreover, local conditions, different practices at the plants, and even the metal variations in the scrap composition, may affect the chemical composition of the generated slag in a significant way [1–6]. The content of CaO plus MgO is usually > 50 wt% (basic slag); lime is added to ensure the basicity of the process, whereas magnesia is present to protect the basic refractories of the ladle lining [1,6]. LFS also has other oxide components such as FeO, SiO_2 and Al_2O_3.

After each casting, the liquid slag is removed from the ladle; its final disposition depends on the logistics of the plant, although a common practice is to deposit the residual solidified slag in transporting pots [6–8]. During cooling of the slag, and depending on its chemical composition and the thermal and other environmental conditions, different solid phases are formed; these phases determine the subsequent behavior of the solidified slag [3,7]. The presence of free lime (CaO) and free magnesia (MgO) leads to an expansive behavior due to their hydration and carbonation by reacting with the environment, which produces significant changes in the solid slag (*weathering*). For instance, these processes tend to pulverize the slag particles. The mineralogical composition of the solid slag strongly depends on the types of steel [6,9], e.g., silicon or aluminum-killed steel: calcium silicates are preferentially formed during cooling in the first case and calcium aluminates in the second case. Both types of compounds also produce alterations in the slag state. Thus, the weathering will depend on the chemical, mineralogical and granulometric characteristics of the slag [1], as well as by the environmental conditions (humidity, temperature, etc.) [10,11].

Due to the large volume of solid LFS produced, its final disposal is a key issue which requires careful attention by the steelmakers. This

* Corresponding author.
E-mail address: agtomba@fi.mdp.edu.ar (A.G.T. Martinez).

https://doi.org/10.1016/j.ceramint.2018.07.128
Received 6 June 2018; Received in revised form 11 July 2018; Accepted 13 July 2018

situation has stimulated the search for alternatives regarding slag reuse [3,12–14], such as land pH conditioning, road construction, etc. In any case, slag must be ground or milled to reach the desired granulometry. This operation demands time, specific equipment and energy consumption. If the grinding step can be helped by natural weathering, the feasibility of slag recycling will be strongly increased. For that reason, a deeper knowledge of the degradation mechanisms behind weathering is useful. Furthermore, slag weathering mechanisms are critical for understanding other steelmaking processes in which the slag is deeply involved. One example is the protective role of remaining thin slag layers against decarburation of ladle or converter working lining bricks during the steelmaking process [12,15].

In this work, the degradation of a typical steelmaking ladle slag as weathering time increases is studied. On the basis of the available literature and previously reported slag degradation patterns, several experimental techniques, including some which have been little explored before, are used to monitor the evolution of the solid slag as weathering time increases. Details regarding the weathering mechanisms of the complex mix of phases constituting the solid slag have been inferred from the analysis of the experimental data.

1.1. Degradation mechanisms of the steelmaking slags

The main processes which affect the volumetric stability of LFS and cause its degradation are the phase transition of the dicalcium silicate (β-Ca_2SiO_4, C_2S) taking place during cooling, and the hydration and carbonation of free lime and free magnesia by its reaction with the ambient atmosphere [1,6,7,14]. It has long been known that free lime can hydrate expansively and break the slag particles in small fragments within a fairly short time; the same occurs with magnesia particles, with larger expansion but at a slower rate [12,14]. Additionally, the hydration of calcium aluminates could also affect the structural stability of slag particles due to the stepped loss of water [6], but less information about its effect on slag degradation is available. Table 1 summarises the reactions involving these phases, together with their volumetric and mass variations [2,14,16,17].

Besides the chemical and mineralogical compositions, other factors affecting slag stability are: granulometric characteristics, particle porosity, cooling conditions, ambient temperature and humidity, among others [6,18,19].

1.1.1. Reactions of CaO and MgO

Undissolved CaO is the primary source of free lime in solid LFS; in addition, secondary CaO is formed during cooling due to the dissociation of the tricalcium silicate (Ca_3SiO_5, C_3S) [6,14]. Free lime hydrates quickly with rain or ambient humidity, generating hydrated lime or portlandite ($Ca(OH)_2$). The volume occupied by portlandite is larger than that of calcia (100% variation in volume, Table 1) and the hydrated particles grow in a preferred orientation, creating pressure around them [9]. As a consequence, the particles shatter and produce smaller fragments [10]. The interstices or pores make the entry of water into the lime aggregates easy, thus speeding the hydration process [6]; however, the presence of free space where the hydrates can expand may reduce the global volumetric variations associated with the hydration [19]. Moreover, the hydration of free lime with water vapor is more expansive than that produced with the liquid; it appears that some solution and transport of material takes place when liquid is present, distributing the hydroxide and its effect throughout a larger volume [10].

Later, when the calcium hydroxide is in contact with the atmospheric CO_2, both react to form $CaCO_3$ (calcite or vaterite), with a very small increase in volume (Table 1) [11]. The carbonate is the final state of the disintegration of free lime, and when carbonation is complete, the slag can be considered volumetrically stable [1].

The hydration process of periclase (MgO), similar to that of CaO, also involves volumetric instability, but it takes place more slowly, causing slag to fragment after months or even years [9,14]. The periclase transforms to $Mg(OH)_2$ (brucite), with a 120% change in volume (Table 1),which is even higher than that of lime. Brucite is carbonated by reaction with the atmospheric CO_2 to form $MgCO_3$ (magnesite), with a small increase in volume (15%, Table 1). The combined effects of the hydration and carbonation of magnesia usually produces hydromagnesite ($Mg_5(CO_3)_4(OH)_2{\cdot}4H_2O$) [6]. As in case of lime, the presence of magnesite or hydromagnesite represents the final state of MgO's reaction with the environment [1].

1.1.2. Reactions of calcium aluminates

The calcium aluminates present in steelmaking slags, mainly celite (C_3A) and mayenite ($C_{12}A_7$) [2], undergo a complex and fast hydration process [17], which can be completed in days [14]. The products of the first step are mixes of CAH_{10} and C_2AH_8 unstable gels, and hydrated alumina (AH_3), which also forms an amorphous gel. This process is exothermic and expansive; the products cover the particles, creating a linking effect between them (hydraulic bond) in which the cementitious characteristics of the aluminates are based.

The second stage of hydration is *nucleation*, which occurs faster than the initial step [17]. CAH_{10} (hexagonal, metastable) forms first, at lower temperatures, and then evolves into C_2AH_8 (pseudo-hexagonal). Between 10 and 27 °C, both hexagonal hydrates may be formed [20]. As time passes or with increased temperature, the transformation to C_3AH_6, the only stable hydrate, takes place. Then, it crystallizes in a cubic system (*conversion* process) accompanied by the formation of gibbsite (crystalline form of AH_3) [17,21]. The first hydration steps are accompanied by the formation of CaO and AH_3 (Table 1), whereas the transformations between hydrates involve the release of water. Due to the lower proportion of CaO present in its formula, $C_{12}A_7$ (mole CaO/Al_2O_3 = 1.3) hydrates more slowly than celite [20] and forms a higher amount of hydrated alumina gel and gibbsite. The presence of the stable hydrate C_3AH_6 is associated with the final stage of hydration.

The subsequent reactions with water are accompanied by volumetric variations (Table 1): the first step is expansive (formation of CAH_{10} and C_2AH_8 gels), and then significant shrinkage takes place (formation of C_3AH_6) [14,16,17]. Taking these changes into account, the most harmful process would be this last step, when an increase in porosity and a loss of mechanical strength is created, thus favoring crumbling. Conversely, the expansive stage is produced with the formation of gels, with the volumetric variation likely to be less severe; this situation, together with the hydraulic bonding (cementitious action) could favor the agglomeration of the slag particles [20,21].

Table 1
Reactions involved in slag degradation.

Reaction		Variation	
		vol%	wt%
$CaO(s) + H_2O(l, g) \rightarrow Ca(OH)_2(s)$	(1)	100	32
$Ca(OH)_2(s) + CO_2(g) \rightarrow CaCO_3(s) + H_2O(l, g)$	(2)	10	35
$MgO(s) + H_2O(l, g) \rightarrow Mg(OH)_2(s)$	(3)	120	45
$Mg(OH)_2(s) + CO_2(g) \rightarrow MgCO_3(s) + H_2O(l, g)$	(4)	15	45
$C_3A(s) + 10H(l, g) \rightarrow CAH_{10}(s) + 2C(s)$	(5)	65	65
$C_{12}A_7(s) + 48H(l, g) \rightarrow 6C_2AH_8(s) + A(s)$	(6)	95	60
$2CAH_{10}(s) \rightarrow C_2AH_8(s) + AH_3(s) + 9H(l, g)$	(7)	− 40	− 25
$3C_2AH_8(s) \rightarrow 2C_3AH_6(s) + AH_3(s) + 9H(l, g)$	(8)	− 30	− 15

C = CaO; A = Al_2O_3; H = H_2O.

2. Materials and methods

This study was done using a batch of ~ 20 kg of used air-cooled ladle slag from steelmaking melts (Fig. 1).

The as-received batch was divided into four granulometric fractions (GF) by using ASTM sieves: a) < 1.4 mm (No. 14 mesh); b) between 1.4

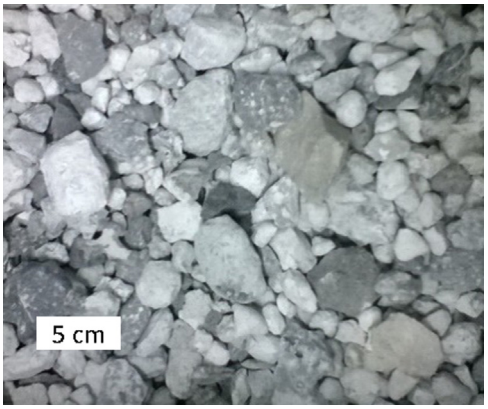

Fig. 1. As-received LFS sample.

and 4.0 mm (No. 14–5 mesh); c) between 4.0 and 7.2 mm (No. 5–3 mesh); and d) > 7.2 mm (No. 3 mesh). These granulometric fractions were named GFff (very fine), GFf (fine), GFc (coarse) and GFcc (very coarse), respectively. Impurities such as iron and/or steel particles coming from the metallic melt were separated from GFcc and GFc by a magnetic method; the total extracted mass measured ~ 150 g and, considering its magnetic properties and X-ray diffraction analysis, was determined to be mainly iron based phases. However, not all the iron-containing phases could be removed from the slag batch, since some of these particles were localized in the slag aggregates and were detected only after their crumbling.

The time when the study began was considered as the 'zero point' (t = 0): from this moment, samples of each GF were extracted at different sampling time. The evaluation of the four granulometric fractions was done after 1, 3, 7, 21, 35, 49, 70 and 126 days from the zero point in order to monitor the slag degradation (weathering) at room temperature (between 15 and 20 °C) under ambient conditions (relative humidity ~ 80%). For that purpose, the following characterization techniques were selected: a) particle size distribution (granulometry) by sieving; b) mineralogical composition by X-ray diffraction (XRD); c) chemical composition by X-ray fluorescence (XRF); d) thermal differential (DTA) and thermogravimetric (TGA) analyses. Except for the granulometric analysis, powders (< 210 μm) of each GF obtained using a planetary mill (Planetary - Micro Mill "Pulverisette 7" Fritsch, Germany) at 505 rpm for intervals of 5 min and a manual impact mortar of tungsten carbide, were analyzed.

The granulometric evolution of each fraction was examined using the same ASTM sieves employed for the initial separation (No. 3, 5 and 14 meshes). Since the extraction of samples for further analysis (by XRD, XRF and DTA/TGA) modifies the granulometric evolution of each GF, a correction to their masses was made. Several alternatives for masses correction were previously analyzed: a) do not make any correction to the total mass of each GF, b) normalize the total mass of each GF in every sampling time with the value at 126 days, c) normalize the total mass of each GF in every sampling time with the value at zero point and d) add the extracted mass to the total mass of each granulometric fraction in every sampling time as an inert material. The latter was the method used to correct GF's masses, because the other three alternatives led to inconsistent results. Mineralogical composition was analyzed by XRD using a Philips Analytical PW 1830/40 diffractometer (The Netherlands), with 40 kV, 30 mA and Cu radiation (K_α = 1.5418 Å). X-ray patterns were acquired from 10° to 75° 2θ with a step of 2°/min. Chemical composition was determined by XRF using a Thermo Electron ARL model 9900 (USA). Thermal analyses (TGA and DTA) were performed at 10 °C/min up to 1000 °C in air flow with a Shimadzu TGA-50 (Japan) and a Shimadzu DTA-50 (Japan), using Pt cells and alumina as reference.

3. Results and discussion

3.1. Granulometric evolution

As was previously mentioned, the slag particles tend to fracture due to the expansive reactions occurring during weathering [6,8,10]. The slag then becomes finer, with a change in its particle size distribution. For this reason, the analysis of the evolution of granulometry is considered a good indicator of slag degradation.

Granulometric evolution represented as the weight percentage of each GF with respect to the weight of the entire slag batch (19.5 kg) is shown in Fig. 2. At the zero point, the proportions of each fraction were: 57.6 wt% of GFff, 12.1 wt% of GFf; 6.9 wt% of GFc; 23.3 wt% of GFcc. A higher proportion of fines is typical of white slags [6]; this characteristic increases the chances of reusing the slag as cement, although it makes its manipulation and use as inert aggregates difficult [3].

Due to the degradation process, particles in the size range of GFcc (> 7.2 mm) became finer and then, the mass of this fraction tended to reduce for longer sampling times, which explains the changes of this GF in Fig. 2. Conversely, the amount of particles in the size range of GFff (< 1.4 mm) increased because this fraction received fragments of particles from all the other fractions due to their crumbling. At the end of the sampling (126 days), GFff increased 2.8% and GFcc decreased 2.3% with respect to their original weights. As can be observed, GFcc and GFff exhibit a quite symmetric change in mass. On the other hand, the intermediate GFf and GFc may lose or gain mass. In this case, a slight tendency to lose mass prevailed in both granulometric fractions after the first 7 days.

These results show that GFcc particles suffered mainly from surface pulverization by weathering; this produces very fine particle fragments (dust) which fall directly into GFff instead of fracturing into a few fragments across the hydrated (or carbonated) surface layer. The same process probably took place in the other two intermediate GF, which explains their tendency to lose mass as well as the higher variation in the proportion of very fine particles (GFff).

Curves in Fig. 2 also show a higher slope at the beginning of the sampling. This was attributed to the fact that surface hydration during reactive phases is expected to be already present before the zero point of the weathering test. Friction during sieving could help detach the previously hydrated and degraded layer of the particles. This can explain the initial higher rate of weight mass changes that are observed in all the samples, but mainly in GFcc and GFff. Subsequently, when sampling frequency decreased, and the sieving operation interfered to a lesser extent with the superficial dust detachment, the rate of change

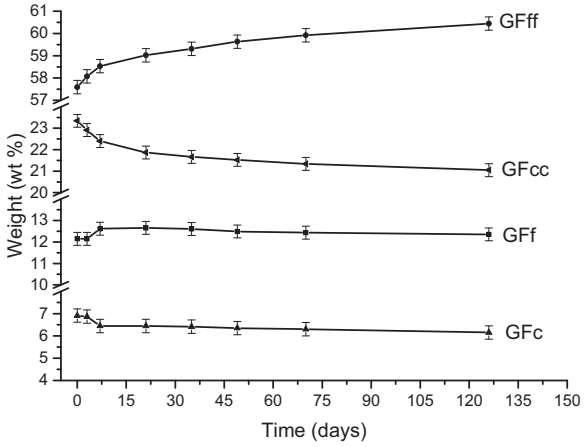

Fig. 2. Evolution of granulometric fractions (as the percentage of the total slag sample).

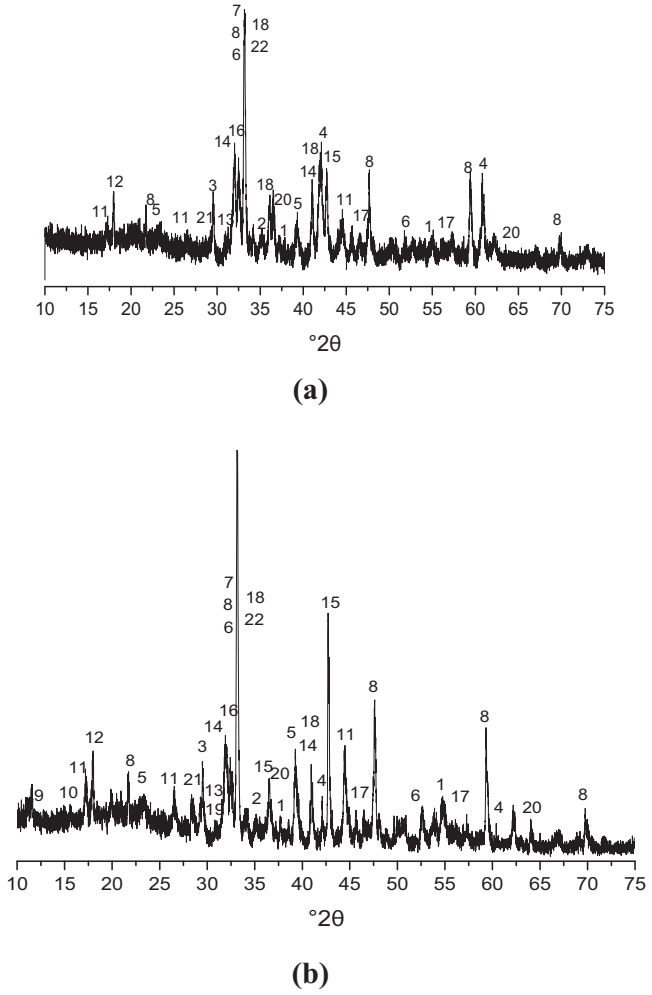

Fig. 3. Diffractograms of GFcc (a) and GFff (b) at the beginning of sampling (references in Table 2).

became stable and the evolution of the granulometric distribution is then considered to be more representative of the degradation rate of each fraction. The moment when rate stabilization took place was around 21 days after the zero point.

3.2. Chemical and mineralogical evolution

The diffractograms of GFcc and GFff powders at the beginning of the sampling are shown in Fig. 3. The crystalline phases identified are listed in Table 2; the number of dots represents the relative amount of each phase.

Numerous crystalline phases were determined in both granulometric fractions, in agreement with those reported in the literature for steelmaking ladle slags [3,4,9,14,18]. The presence of free CaO and MgO was confirmed in both GFs, together with calcium aluminates such as celite ($Ca_3Al_2O_6$, C_3A) and mayenite ($Ca_{12}Al_{14}O_{33}$, $C_{12}A_7$). Intense XRD peaks of $MgAl_2O_4$ spinel were also identified in both GFs, and in similar amounts. Minor Si-containing phases such as Ca_2SiO_4 and other ternary and quaternary compounds were detected, as well as oxide and other solid phases containing iron. These Fe-components could come from the metallic melt that is incorporated in the slag; the content of these phases seems to be higher in GFcc.

Furthermore, hydrated as well as carbonated phases (from CaO, MgO and calcium aluminates) were identified mainly in GFff (indeed, none of the carbonates were detected in GFcc). This fact confirms that the slag was already degraded at zero point, in agreement with previous results of similar steelmaking slags after one day of weathering [1]. The particular distribution of the degraded phases is due to different reasons. First of all, the inherent higher reactivity of finest particles, and the pulverization derived from the hydration processes. Moreover, the free lime and periclase present as coarser particles are likely mixed with and hindered by other solids, which slow the reactions with vapor water and atmospheric CO_2 [14].

In the case of calcium aluminates, they were also found in higher proportion in GFff. Moreover, the presence of phases corresponding to the products of the first step of hydration, CAH_{10} and C_2AH_8, as well as C_3AH_6 formed at the final stage of the process, was detected. This finding is in agreement with the high speed of these reactions [1], even when the amount of water was limited (it only corresponded to the environmental moisture, which was also consumed in the other hydration processes). The absence of hydrated compounds in the coarsest granulometric fraction is attributed to the following reason. The calcium aluminate particles in GFcc more prone to react with water were the smallest ones; moreover, as soon as they hydrated, the conversion process (formation of C_3AH_6), which is considered the most disruptive step, leading to pulverization, took place. As a consequence, the hydrates tended to pass to finer GF, being undetectable by XRD in GFcc.

The mineralogical compositions of GFf and GFc were intermediate between the coarsest and finest granulometric fractions; for instance, XRD peaks of the main hydrated phases such as $Mg(OH)_2$ were identified with lower intensities than those of GFff.

The proportions determined by XRF of the main chemical components of a typical slag in the middle of the ladle campaign are shown in Table 3 (expressed as oxides). These values can be considered as a rough estimation of the composition of the slag batch at the zero point. Other minor compounds (< 3 wt%) present as a consequence of steel cleaning (not shown), are: FeO_x MnO, S, and Cr_2O_3. The ternary basicity of this slag, calculated as a $CaO/(Al_2O_3 + SiO_2)$ weight ratio, is 1.7. This lowest basicity ratio is the reason for the high proportion of mayenite and tricalcium aluminate present as $CaO\text{-}Al_2O_3$-containing phases in the slag (Table 2), in agreement with what was indicated by Posch et al. [2]. XRF data for each GF after 21 and 126 days of weathering are also shown in Table 3.

Values of Table 3 show that higher amounts of Al- and Ca-containing phases are present in the finer granulometric fractions. The content of aluminum (informed as Al_2O_3) corresponds to the higher proportion of anhydrous calcium aluminates plus the hydrated phases initially identified only in GFff. Similarly, a concentration of CaO in the finer GF was observed since calcium is part of these aluminates, and a higher proportion of $CaCO_3$ and $Ca(OH)_2$ were identified by XRD as the particle size of the GF becomes smaller. As a consequence, the proportion of the other components, such as Si, follows the opposite tendency. This could be also the reason why MgO is distributed in similar proportions in all the fractions even though a higher amount of this component in the finer GF was expected considering the XRD analysis. Moreover, the low content of magnesia in the global slag composition may also produce small changes of its content in each GF, in the order of the error of the XRF technique (around 0.5–1% [22]).

Regarding the evolution over time, the chemical composition of each GF was rather stable throughout the sampling time, as can be inferred from the XRF data in Table 3.

Due to the overabundance of different compounds present in the slag, only the main phases are analyzed in relation to their evolution during the sampling time. As an example, Fig. 4 shows the XRD patterns of the four granulometric fractions obtained at 21 and 126 days after the zero point. In Fig. 5, the XRD patterns of the two extreme granulometric fractions (GFff and GFcc) from 3 (21 days) to 18 (126 days) weeks of weathering are shown together.

In what follows, the analysis will be focused only on those phases that are mainly involved in slag degradation (Table 1), corresponding to the first twelve phases of Table 2: a) CaO, Ca(OH) and $CaCO_3$ (reactions (1) and (2)); b) MgO, $MgO(OH)_2$ and $MgCO_3$ (reactions (3) and

Table 2
Crystalline phases detected by XRD in GFcc and GFff (zero point).

IDCC file no.	Mineral phase	Formula	Code[a]	GF	
				GFff	GFcc
00-043-1001	Lime	CaO	1	–	*
01-072-0156	Portlandite	$Ca(OH)_2$	2	**	*
01-083-0577	Calcite	$CaCO_3$	3	****	*
01-071-1176	Periclase	MgO	4	*	**
01-082-2454	Brucite	$Mg(OH)_2$	5	**	*
00-003-0788	Magnesite	$MgCO_3$	6	***	–
00-048-1882	Mayenite	$Ca_{12}Al_{14}O_{33}$ ($C_{12}A_7$)	7	****	**
00-001-1060	Celite	$Ca_3Al_2O_6$ (C_3A)	8	****	***
00-012-0408	Caldecahydrite	$CaAl_2H_{20}O_{14}$ (CAH_{10})	9	*	–
00-045-0564	Calcium Aluminum Oxide Hydrate	$Ca_2\ Al_2H_{16}O_{13}$ (C_2AH_8)	10	*	–
01-074-2281	Katoita	$Ca_3Al_2(OH)_{12}$ (C_3AH_6)	11	***	–
00-012-0460	Gibbsite	$Al(OH)_3$	12	***	**
01-075-1655	Dolomite	$CaMg(CO_3)_2$	13	*	*
00-033-0302	Larnite/belite	Ca_2SiO_4	14	***	–
01-074-1883	Wuestite	FeO	15	**	**
00-032-0469	Hematite	Fe_2O_3	16	*	**
00-001-1295	Pyrite	FeS_2	17	*	*
00-035-0591	Merwinita	$Ca_3MgSi_2O_8$	18	**	**
00-035-0133	Preocroite	$Ca_{20}Al_{26}Mg_3Si_3O_{68}$	19	–	*
01-075-1800	Spinel	$MgAl_2O_4$	20	**	**
01-078-1391	Pyroxene	(Ca,Mg,Fe) SiO_3	21	*	–
01-079-1657	Andradite	$Ca_3Fe_2(SiO_4)_3$	22	**	*

[a] Code reference for Figs. 3, 4 and 5.

Table 3
XFR chemical compositions (main components) of slag samples.

Sampling time	GF	Moles percentage (mol%)			
		CaO	Al_2O_3	SiO_2	MgO
~ Zero point	–	63	16	9	12
21 days	GFff	64.7	14.4	9.9	11.0
	GFf	62.8	14.2	10.6	12.4
	GFc	62.5	13.5	11.9	12.1
	GFcc	61.6	10.4	16.1	11.9
126 days	GFff	64.7	14.5	10.6	10.3
	GFf	61.1	12.9	13.3	12.7
	GFc	61.3	10.8	15.8	12.1
	GFcc	60.7	10.6	16.6	12.1

(4); c) C_3A, $C_{12}Al_7$, CAH_{10}, C_2AH_8, C_3AH_6O and $Al(OH_3$ (reactions (5)–(8)). Changes related to the hydration of Ca_2SiO_4 were dismissed in the analysis due to the small amount of this silicate and its low inherent reactivity with environmental humidity [1,14].

Initially (zero point, Table 2), there was mainly free lime in the coarsest fraction whereas this phase cannot be clearly identified in GFff. The CaO was already hydrated by water vapor (before the beginning of the sampling) to form the hydroxide, which was detected mainly in the finest GF; it was principally carbonated here afterwards due to the small size of the particles. This tendency continued as time passed. Free lime was not clearly identified after the third week (21 days) in GFcc, since the amount of $CaOH_2$ in this GF was very low, especially after week 10. Changes concerning CaO-related phases still occurred in spite of the presence of a strong XRD peak of the carbonate at the beginning (Table 2) in GFff. A similar reaction pattern appeared for MgO particles, but at a slower rate: from zero point onwards, free magnesia was always present mainly in GFcc, whereas hydrates and carbonates were concentrated in finer granulometric fractions. Diffraction peaks of periclase continue appearing for sampling times higher than 10 weeks in the coarser granulometric fractions.

In the intermediate GF, GFf and GFc, XRD peaks corresponding to Ca and Mg oxides and their hydrated phases were detected. Their intensities were variable with time: in the first 5 weeks (35 days), an increase of the intensity of hydroxides peaks was observed, with differences between $Ca(OH)_2$ (the increase in intensities was already more accentuated in the first 3 weeks) and $Mg(OH)_2$. However, at longer times, the intensities tended to decrease, with the diffraction pattern at 18 weeks (126 days) similar to that of GFcc. The number of carbonated phases tended to be low in the intermediate GF, and although the intensity of XRD peaks in GFf was relatively higher than that of GFc, they were always lower than those of GFff during the entire the sampling time. This fact confirms that the formation of carbonates took place preferentially once the hydroxide was part of the finest GF due to the higher reactivity of these particles (i.e., the number of carbonates formed by crumbling was quite lower).

Considering the evolution of CaO- and MgO-related phases in every GF, it can be asserted from XRD analysis that at the end of the sampling time, free magnesia did not convert completely into magnesite, whereas conversely, free lime was almost completely transformed into the carbonate. This fact reaffirms that changes related to free lime occur faster than those corresponding to free magnesia, as was previously reported [1,9,11,14].

Meanwhile, XRD peaks of calcium aluminates (anhydrous) were present from the beginning to the end of the test in all the granulometric fractions, indicating that the hydration process was not completed during the tested sampling time. Similar results have been reported by Setien et al. [1] in steelmaking slags with contents of Al_2O_3 around 12–19 wt%. The intensity of the peaks corresponding to the calcium aluminates was higher in the finer GF. This characteristic was maintained in spite of the decrease in the intensity of the XRD peaks corresponding to these phases as a product of their hydration. After 70 days (10 weeks), the amount of non-hydrated aluminates decreased more quickly in the coarser fractions.

Hydrated calcium aluminates appeared from the zero point only in GFff (Table 2) as a band between 10° and 30° 2θ [1,5,17,19], which is typical of solids of low crystallinity and associated with the presence of CAH_{10}, C_2AH_8 and AH_3 gels. This band was observed in GFf diffractograms starting at week 5; the presence of these gels was detected until the tenth week (70 days) of testing in the two finer granulometric fractions, GFff and GFf (less notably in the seventh week for GFff). Later, this band was not identified in any of these cases. The presence of gels was also observed in the coarser granulometric fractions between weeks 7 and 10, with the band being less intense than those of the finer

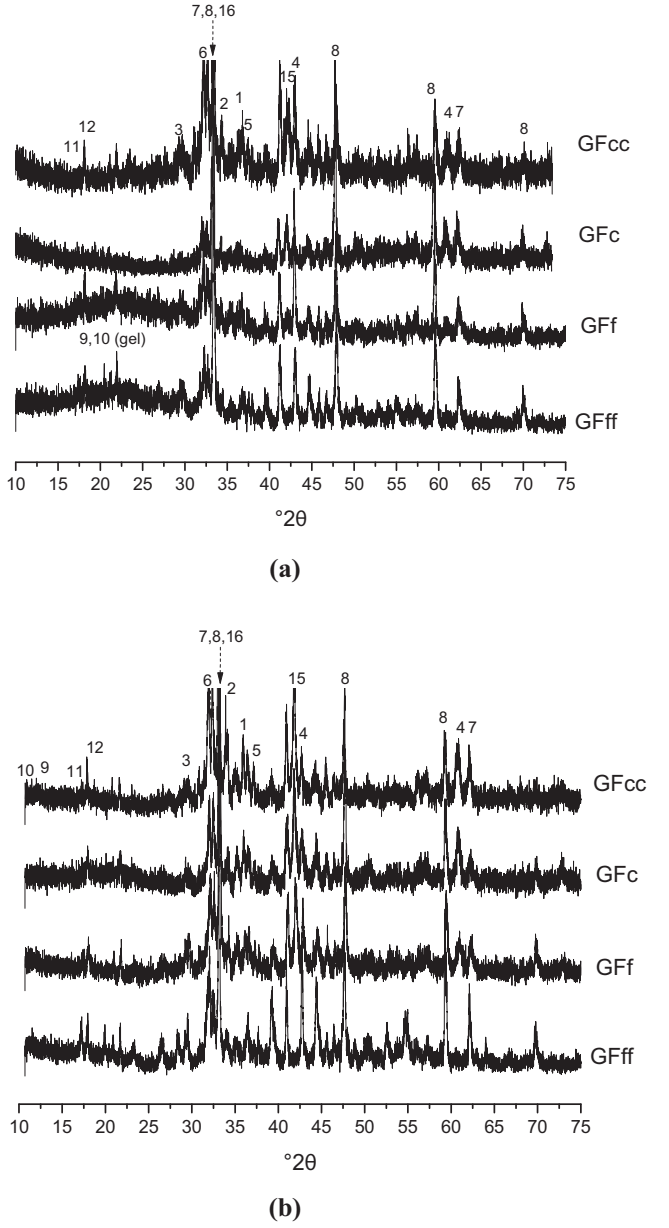

Fig. 4. XRD patterns of granulometric fractions: (a) 21 days (3 weeks) and (b) 126 days (18 weeks).

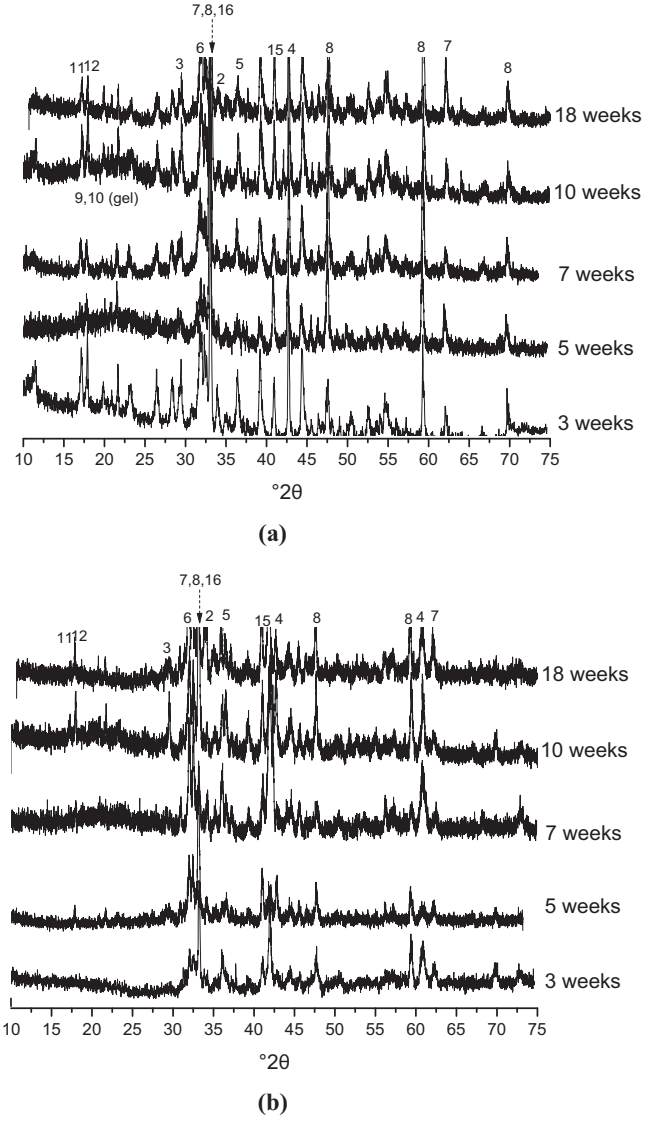

Fig. 5. XRD patterns at different sampling times for: (a) GFff and (b) GFcc.

granulometric fractions; this fact was attributed to the hydration of the calcium aluminates present originally in these fractions and/or to the agglomeration of finer (and more reactive) particles thanks to the cementitious properties of the formed hydrates.

The stable crystalline phases C_3AH_6 and gibbsite (crystalline hydrated alumina) were identified only in the finest GF from the beginning of the sampling, whereas they were only detected starting from the third week in GFf. In the coarser fractions, these solids were identified from week 10 onwards. The absence of the characteristic bands of gels in the diffractograms of the four GFs analyzed after 18 weeks of weathering indicates that most of them crystallized, and these crystalline phases C_3AH_6 and AH_3 were concentrated in GFff and GFf.

The evolution of the mineralogical composition of granulometric fractions throughout the sampling time draws attention to the stability of their chemical composition obtained by XRF (Table 2). This was attributed to the small weight variation determined by granulometry, approximately 2.5 wt% on average, which corresponds to all the phases involved in the chemical composition changes (mainly CaO and the calcium aluminates, and MgO and the carbonated phases in lesser extent), added to the error linked to the sampling and that inherent in the XRF technique (around 0.5–1% [22]). Taking these results into account, this last technique is considered to provide limited information about slag degradation by weathering over time.

3.3. Complementary thermal analysis

Hydrated and carbonated phases are expected to undergo the reverse reactions and lose weight when they are subjected to thermal treatment. For this reason, a set of thermogravimetric analyses (TGA) of all the studied slag samples were performed to complement the XRD analysis. As an example, TGA curves of every GF after 21 and 126 days from the zero point of the weathering test are shown in Fig. 6; differences in curves as a function of the granulometric fraction and sampling time are evident.

Below 350 °C, the main mass variation is associated with the dehydration of pre-hydrated calcium aluminates [14]. Between 350 and 450 °C, the mass change is related to the dehydration of magnesium and calcium hydroxides [1,7]. Finally, above 450 °C, the decomposition of carbonates takes place [1,7]. These reactions were verified by DTA analysis (Fig. 7).

Remarkable weight losses at temperatures lower than 450 °C were

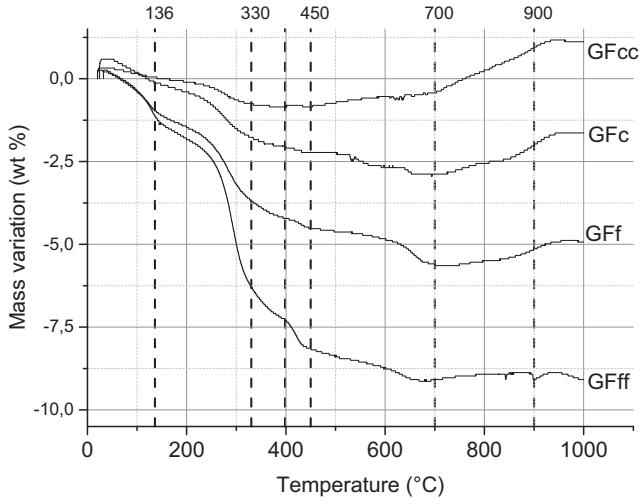

(a)

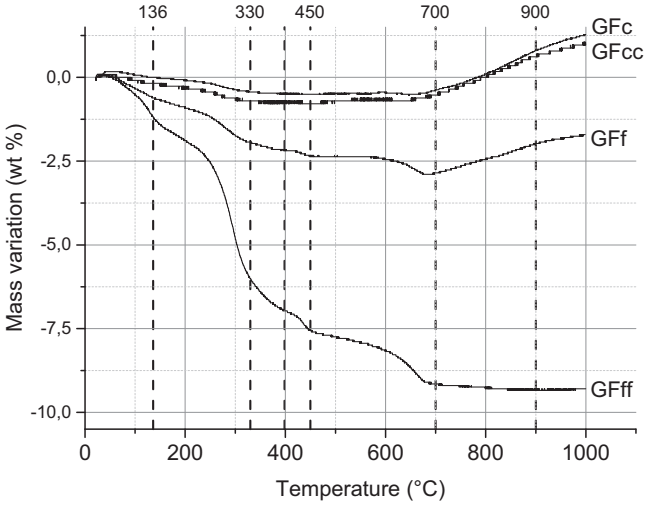

(b)

Fig. 6. TGA curves of each GF after (a) 21 days and (b) 126 days.

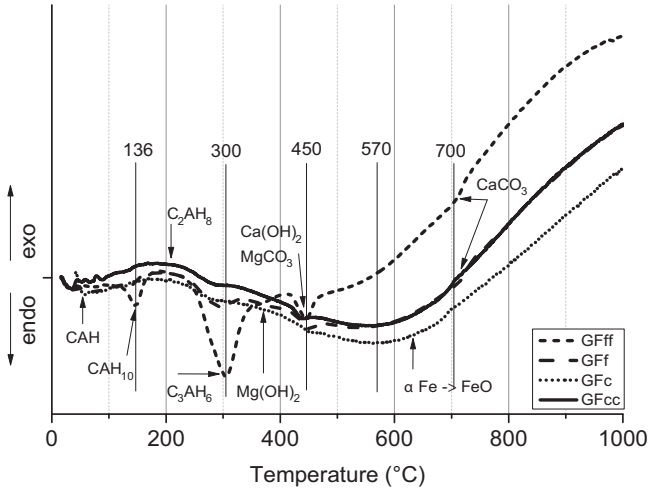

Fig. 7. DTA curves for each GF after 126 days.

observed in the TGA curves, with higher loss in the case of the finest and most degraded fraction GFff, associated with the loss of water of phases such as $Ca(OH)_2$, $Mg(OH)_2$ and hydrated calcium aluminates. Moreover, mass variations in the thermal range associated with hydrated calcium aluminates such as CAH_{10}, C_2AH_8 and C_3AH_6 (130–330 °C) were observed in every TGA curve; this fact confirms the presence of such hydrated phases in all the GFs, which was less clear from XRD patterns in certain cases due to the non-crystalline nature of some of the hydrates.

Comparing results after 21 and 126 days, the mass losses of GFcc and GFff below 450 °C did not change much (although some variations were observed at intermediate sampling times, which are not shown): < 0.1 wt% for GFcc and < 0.5 wt% for GFff. Firstly, this indicates that CaO, MgO and/or calcium aluminates always remain in GFcc to be hydrated during the weathering, and that the hydrated phases pass to the finest fractions at almost the same rate throughout the sampling time (as can be also observed in the granulometric curves in Fig. 2). According to that inferred from the XRD patterns, $Mg(OH)_2$ and the calcium aluminate hydrates coming from the celite and mayenite present in GFcc could be mainly responsible for the mass losses at temperatures < 450 °C after the third week. The slow kinetic of transformation of magnesia to the hydroxide, and the tendency of calcium aluminate hydrates to pass to GFff, especially when gels crystallized, can be reasons for the small variation in the mass losses of GFcc. On the other hand, in the case of GFff, the small variation in mass losses in this range of temperature over a longer sampling time can be associated with two superimposed effects, derived from the mineralogical evolution analysis (XRD): there would have been an increase in the content of the hydroxides (and in mass loss as a consequence) as time passed, but these phases were also carbonated by the CO_2 in the air, consuming them (and reducing the mass loss).

Conversely, the mass losses of the intermediate granulometric fractions below 450 °C decreased over a longer sampling time, becoming more similar to GFcc as the weathering advanced, as was also derived from XRD analysis. This fact agrees with the granulometric evolution, since GFc and GFf tended to lose fines which were mainly constituted by hydrated phases as was inferred from the XRD results. Up until the fifth week, that mainly responsible for the mass loss displayed in TGA curves in the range of temperatures lower than 450 °C would be the portlandite, whose proportion in the intermediate granulometric fractions decreased from this moment; this process would contribute to the reduction of mass loss determined by TGA up to 450 °C. Moreover, between weeks 5 and 7, the calcium aluminate hydrates also contributed to this mass loss, but the carbonation of hydroxides would have the opposite effect. This combination of factors could justify the evolution of this TGA step over longer sampling times.

Considering the thermal region corresponding to dehydration of calcium aluminate hydrates, the highest mass losses from the third week onward were observed between 250 and 300 °C, where C_3AH_6 loses the structural water [1,14], mainly in GFff and GFf. This fact indicates that even when the diffractions peaks of this hydrate were clearly identified starting from week 10 in the coarser fractions (GFc and GFcc), this phase was there before, likely as a solid with low crystallinity (which could make its detection by XRD difficult). In agreement with that observed in the diffractograms of GFff, the mass loss corresponding to the dehydration of C_3HA_6 remained high over the entire sampling time. This confirms the concentration of calcium aluminates in this granulometric fraction and the production of fines during the crystallization stage of this hydrate in the other three coarser fractions. In fact, this TGA step decreased for GFf as time passed.

Meanwhile, the mass variation in TGA curves in this thermal range (250–300 °C) for GFc and GFcc was very small at the beginning and increased slightly until the tenth week (70 days), in keeping with the appearance of diffraction peaks corresponding to calcium aluminate hydrates. Finally, near the end of the sampling, the mass loss decreased again, which can be attributed to pulverization and the fact that there were fewer and fewer non-hydrated calcium aluminates.

TGA mass variations in the thermal range corresponding to the decomposition of carbonates (> 450 °C) confirm that only the finest fractions have an appreciable concentration of these phases, according to that inferred from XRD analysis. At temperatures above 700 °C, the mass increased, mainly in the coarser GF; this behavior is related to the oxidation of Fe-containing phases present as impurities, mainly the metallic iron emulsified with the molten slag.

4. Final considerations

Reaction with the environment (humidity and CO_2) of a particular steelmaking ladle slag was evaluated over 18 weeks. These reactions led to the fast formation of hydrated and carbonated species of Ca and Mg, with corresponding volumetric changes and pulverization. The last process was confirmed by the enrichment of the reactions products in the finest fraction (< 1.4 mm), even when an increase of just of 2.8 wt% was observed during the testing time.

The solid oxide that hydrated faster was free CaO, and it was considered as mainly responsible for the slag pulverization. The contribution of the degradation of free periclase was smaller, due to the smaller amount of MgO in the slag composition and the slower rate of the process related to its reaction with the environment. In spite of the high amount of carbonated species, which are products of the final stage of weathering, the studied slag still manifested intense mineralogical changes during the sampling time.

Other components which underwent significant changes during the weathering are the calcium aluminates, which were already hydrated when the study began due to the reaction with water vapor that began during the first hours of the weathering. The hydration led to the transformation of hydrates into the stable C_3AH_6 phase. An interesting aspect observed during the test was the concentration of both anhydrous and hydrated calcium aluminates in the finest granulometric fraction (< 1.4 mm). At the end of the test, a remarkable decrease in the intermediate hydrated phases (gels) and an increase in the final stage product were observed, although there were un-reacted anhydrous aluminates still after the 18 weeks. Bearing in mind the characteristics of the processes taking place during the hydration, and the degree in which such reactions identified in this study advanced, it can be asserted that the transformation occurring in relation to the presence of C_3A and $C_{12}A_7$ actually led to the generation of fines.

Regarding the experimental methodology used in this work, and considering the information obtained from the applied analytical techniques, the monitoring of particle size evolution turned out to be a good way of evaluating the weathering of the ladle slag. Even though chemical composition data complemented the analysis of the distribution of phases among the different granulometric ranges, the XRF turned out to be a limited technique for evaluating the changes over time. However, the XRD study complemented by DTA/TGA gave very useful information, which allowed us to get a more detailed description about how the transformation of the slag occurred as a consequence of its reactions with the environment.

Finally, it is worth noting that the as-received slag consisted mainly of a fine powder with particles smaller than 1.4 mm, with cementitious properties provided mainly by the presence of anhydrous calcium aluminates. Both characteristics are promising for alternative reusing of the studied ladle slag.

Acknowledgments

This work was carried out under the research project PICT 2012-1215 “Chemical degradation of refractory materials of steelmaking use” founded by the National Agency for Scientific and Technological Promotion (ANPCyT), and within the scope of the CYTED network 312RT0453 (HOREF).

Declarations of interest

None.

References

[1] J. Setien, D. Hernández, J. González, Characterization of ladle furnace basic slag for use as a construction material, Constr. Build. Mater. 23 (2009) 1788–1794.
[2] W. Posch, H. Presslinger, H. Hiebler, Mineralogical evaluation of ladle slags at Voestalpine Stahl GmbH, Ironmak. Steelmak. 29 (2002) 308–312.
[3] C. Shi, Steel slag- Its production, processing, characteristics and cementitious properties, J. Mater. Civ. Eng. (2004) 230–236.
[4] M. Tossavainen, F. Engstrom, Q. Yang, N. Menad, L.M. Lidstrom, B. Bjorkman, Characteristics of steel slag under different cooling condition, Waste Manag. 27 (2007) 1335–1344.
[5] A. Bougara, C. Lynsdale, N.B. Milestone, Reactivity and performance of blastfurnace slags of differing origin, Cem. Concr. Compos. 32 (2010) 319–324.
[6] T.Herrero. Vázquez, Estudio del efecto de la hidratación de la escoria blanca de acería de HEA: aplicación en pastas y morteros de cemento. Tesis doctoral, Escuela Técnica Superior de Ingeniería, Bilbao, 2015.
[7] J. Waligora, D. Bulteel, P. Degrugilliers, D. Damidot, J.L. Potdevin, M. Measson, Chemical and mineralogical characterizations of LD converter steel slags: a multi-analytical techniques approach, Mater. Charact. 61 (2010) 39–48.
[8] G. Wang, Y. Wang, Z. Gao, Use of steel slag as a granular material: volume expansion prediction and usability criteria, J. Hazard. Mater. 184 (2010) 555–560.
[9] I.Z. Yildirim, M. Prezzi, Chemical, mineralogical, and morphological properties of steel slag, Adv. Civil Eng. (2011) (Article ID 463638).
[10] L.M. Juckes, The volume stability of modern steelmaking slags, Mineral Process. Extr. Metall. (Trans. Inst. Min. Metall. C) 112 (2003) C177–C197.
[11] J.M. Manso, M. Losañez, J.A. Polanco, J.J. Gonzalez, Ladle furnace slag in construction, J. Mater. Civ. Eng. 17 (2005) 513–518.
[12] R. Dippenaar, Industrial uses of slag (the use and re-use of iron and steelmaking slags), Ironmak. Steelmak. 32 (2005) 35–46.
[13] H. Yi, G. Xu, H. Cheng, J. Wang, Y. Wan, H. Chen, An overview of utilization of steel slag, Procedia Environ. Sci. 16 (2012) 791–801.
[14] V. Ortega-Lopez, J.M. Manso, I.I. Cuesta, J.J. Gonzalez, The long-term accelerated expansion of various ladle-furnace basic slags and their soil-stabilization applications, Constr. Build. Mater. 68 (2014) 455–464.
[15] A. Gimenez, L. Musante, M. Zurzolo, C. Capurro, C. Cicutti, P. Galliano, Ladle thermal conditions during long non-working periods: impact on lining performance, Steel Conference IAS (Rosario, Argentina, November 2016), 2016.
[16] Y. Iguchi, T. Narushima, C. Izumi, Calorimetric study on hydration of CaO-based oxides, J. Alloy. Compd. 321 (2001) 276–281.
[17] J.M. Rivas Mercury, A.H. De Aza, X. Turrillas, P. Pena, Hidratación de los cementos de aluminatos de calcio, Bol. Soc. Esp. Ceram. Vidr. 42 (2003) 269–276.
[18] D. Adolfsson, R. Robinson, F. Engström, B. Björkman, Influence of mineralogy on the hydraulic properties of ladle slag, Cem. Concr. Res. 41 (2011) (865–571).
[19] I. Papyianni, E. Anastasiou, Effect of granumoletry on cementitious properties of ladle furnace slag, Cem. Concr. Compos. 34 (2012) 400–407.
[20] C. Parr, F. Simonin, B. Touzo, C. Wöhrmeyer, B. Valdeliévre, A. Namba, The impact of calcium aluminate cement hydration upon the properties of refractory castables, Technical Paper, Kerneos aluminates technologies, TP-GB-RE-LAF-043, 1–17 (TARJ, Japan, September, 2004.
[21] N. Schmitt, J.F. Hernandez, V. Lamoura, Y. Berthaud, P. Meunier, J. Poirier, Coupling between kinetics of dehydration, physical and mechanical behaviour for high alumina castable, Cem. Concr. Res. 30 (2000) 1597–1607.
[22] R.M. Rousseau, Detection limit and estimate of uncertainty of analytical XRF results, Rigaku J. 18 (2001) 33–47.